Supplementary Information of Manuscript entitled: **"Label free nano-aptasensor for interleukin-6 in protein-dilute bio fluids such as sweat.**" authored by L.S. Selvakumar [a], Xiao Wang,[b] Joshua Hagen,[c] Rajesh Naik [c], Ian Papautsky,[b] and Jason Heikenfeld*[a *] submitted to Analytical Methods.

A brief review of IL-6 sensors is provided. Jian-Jun Shi et al., fabricated an ultra sensitive multi- analyte electrochemical immunoassay based on GNR-modified heated screen-printed carbon electrodes and PS@PDA-metal labels in which IL-6 is detected with limit of 0.1 pg/ml. [1] Gao-Chan et al., fabricated a photo chemical immunoassay for sensitive detection of IL-6 based on TiO2/CdS/CdSe dual co-sensitized structure with a detection limit of 0.38 pg/ml. [2] Ting yang et al., fabricated an ultrasensitive platform based on Au nanoparticles deposited on horizontally aligned single walled carbon nanotube array, in situ prepared on a SiO2/Si substrate with detection limit of 0.01 fg/ml in serum. [3] Wang et al. fabricated a highly sensitive IL-6 amperometric immunosensor based on polydopamine, with a linear response range of IL-6 from 4.0 to 8.0 × 10^2 pg/ml and with a low detection limit of 1.0 pg/ml obtained by amperometry. [4] Yang and Li used ferrocene loaded porous polyelectrolyte nanoparticles as a label to detect oral cancer biomarker IL-6, and their immunosensor displayed high sensitivity, wide linear range (0.002–20 ng/ml), low detection limit (1 pg/ml) and good reproducibility.[5] A silver nanoparticle–hollow titanium phosphate sphere hybrid was synthesized by Peng et al. used as a label for electrochemical detection of human IL-6, with extremely sensitive response to IL-6 in a linear range of 0.0005–10 ng/ml and a detection limit of 0.1 pg/ml.[6] ELISA has long been used for clinical protein determinations[7], it's sensitivity is low and it suffers from interference issues which cannot be neglected. LC-MS-based proteomics are expensive and technically complex for clinical diagnostics.[8,9]

Experimental

Materials and reagents

Recombinant Human Interleukin-6 (IL-6, *M*w = 23,718 g mol−1), was purchased from Thermo Scientific™ Pierce™, USA. Reactant free 5 nm diameter gold nanoparticles (AuNPs) with OD 1, stabilized suspension in 0.1 mM PBS were purchased from Sigma (St. Louis, MO, USA). Bovine serum albumin (BSA) was purchased from Sigma (St. Louis, MO, USA). Potassium ferricyanide $K_3[Fe(CN)_6]$ and Phosphate buffer saline powder were purchased from Thermo Scientific™ Pierce™, USA. Commercial artificial sweat was purchased from Pickering Laboratories, In., (California, USA).

DNA Aptamer

All of the modified DNA Aptamers against Human protein Interleukin 6 were obtained from Base Pair Biotechnologies, Inc, Houston, Texas, USA. These include a 5′-$HS(CH_2)_6$-$OP(O)_2O$-$(CH_2CH_2O)_6$-TTTTT-Aptamer sequence for Electrochemical impedance spectroscopy measurement and 6-fluorescein amidite (6-FAM) fluorophore tagged at 5' and Black Hole Quencher (BHQ-1) at the 3' terminal of the

Interleukin 6 aptamer for the molecular beacon assay. An IL-6 binding ssDNA aptamer was first modified by incorporation of oligo ethylene oxide and extension with a poly-T tail (T5) for flexibility, and -(CH_2)- greater linker was labeled with thiol to immobilize it on the AuNPs-modified gold electrode. The length of DNA aptamer is 32 bases with a Kd of 19±4.5nM.

A stock solution of IL-6 was prepared by dissolving 10µg of IL-6 in binding buffer (1X PBS, pH = 7.4, 1 mM $MgCl_2$, and 0.05% Tween) followed by further concentration dilution in binding buffer. Once the aptamer is in working concentration, it needs to be folded by heating in a solution of binding buffer at 85-90 °C for 2 minutes and then cooled to room temperature before use. A stock solution of 100µM DNA aptamer and functionalized aptamer as well as further dilutions was prepared in binding buffer. Stock solutions of DNA were prepared with PBS solution (pH 7.4) and stored in a 4°C freezer.

Apparatus

Electrochemical impedance spectroscopy is used in the characterization of membrane capacitance, resistance, dielectric constant, and surface homogeneity. Electrochemical measurements were performed on a Gamry Reference 600 potentiostat (Gamry Instruments, Warminster, PA, USA) workstation equipped with EIS 300 software. All experiments were carried out using a conventional three-electrode system. A Gold electrode (d = 1 mm) was the working electrode, Pt wire the counter electrode (d=1.6mm) and leakless Ag/AgCl as the reference electrode. Measurements were carried out using a three-electrode system in a 3 mL one-compartment electrochemical cell (Echem Electrode Kit/ref. ET014 and ET080- 12, eDAQ Products, Poland). All potentials were referenced to this reference electrode. A 60 micro well plate Varian Cary Eclipse fluorescence spectrophotometer was used to obtain the emission spectra. Emission spectra on a droplet were obtained using a 6-around-1 fibre optic bundle laser (441.6 nm HeCd model 1K4153R-C; Kimmon Electric Co.), light control modules (shutter, attenuator and focusing optics), a monochromator (0.3 m focal length, triple grating turret) and photon-counting phototube (Acton Research Corp.), and a computer with data acquisition and analysis software (NCL and Spectra-Sense software; Acton). All experiments were carried out at room temperature (20°C). TEM images were recorded with a Philips CM 20 transmission electron microscope with EDS (EDAX/4pi) system (Koninklijke Philips Electronics, Eindhoven, The Netherlands) operating at 220KV. The samples were mounted on formvar-coated on 2-3nm Au on a 400 mesh Au TEM grid.

Design and fabrication of aptamer-based biosensor

The biosensor was fabricated by two steps including an electrochemical surface preparation step and an immobilization step. The 1 mm diameter gold surface was polished with 0.3 μm alumina slurry and then ultra-sonicated in water for 5 min. The procedure for the deposition of gold nanoparticles (AuNPs) at the gold working electrode was adapted from literature[10]. The electrode was then immersed into 0.1M H_2SO_4 solution containing 5nm (0.3mM) AuNPs, and electrochemical deposition of AuNPs was conducted by electrochemically scanning the electrode between a potential of −200 mV and −190 mV (versus SCE) for a selected number of times at a scan rate of 50 mV/s.

For immobilization of the aptamer, the electrode was incubated in 10-μL (1 μM) aptamer in an immobilization buffer solution (I-B) of 10mM Tris–HCl, pH 7.4, 100mM NaCl, and 1mM $MgCl_2$, for 1 h at 100% humidity. The electrode was then washed with deionized water, followed by drying under a N_2 stream. Prior to the use of the IL-6 aptamer, the aptamer (1μM) including 1mM TCEP in I-B was used to reduce disulfide bond oligos by heating to 90°C for 6 min and then gradually cooling to room temperature. This heating and cooling step is essential to maintain the structural flexibility of the aptamer for binding IL-6 [11]. Nonbinding aptamers were removed by rinsing with I-B and deionized water. The resulting electrode was employed as an aptasensor.

10 μL of a fixed concentration of IL-6 was dropped onto the fabricated EIS aptamer-based biosensor, and allowed to interact with 1μM concentration of aptamer with IL-6 for 60 min. It was rinsed completely with 0.1M sodium phosphate buffer (pH-7.4) to remove physically absorbed aptamer and dried by N_2, and then placed into an electrochemical cell. EIS measurement was performed in 2.0ml of 0.1M PBS (pH 7.4) containing 5 mM of $K_4Fe(CN)_6$ redox couple. It should be noted, that the redox couple such as methylene blue and ferrocene can also be attached to the Aptamer, as demonstrated for thrombin protein. [12,13] This would be advantageous as no-sample pretreatment would be needed. The amplitude of the applied sine wave potential in each case was 5 mV, whereas +0.20 V of the direct current potential was limited to the formal potential of the redox couple $Fe(CN)_6]^{3-/4-}$. The electrochemical impedance spectra were recorded within the frequency from 1 MHz to 1.0 Hz with a sampling rate of 10 points per decade. The concentration of IL-6 was quantified by the change of electron transfer resistance of the biosensors as shown in scheme.1a.

Optimization of Aptamer concentration for beacon assay

In order to determine the binding concentration of aptamer with IL-6 protein, fluorimetric assays were carried out. Various concentrations of aptamers ranging from 0.01μM to 0.5μM were added to a constant amount of IL-6 protein in optimized buffer, and excited at a wavelength of 497nm with the emission at 520nm as shown in scheme 1b.

Cyclic Voltammetry of the Electrode Surface of AuNPs/GE

Figure S1 shows cyclic voltammograms (CVs) of the bare gold working electrode (Au) and AuNPs deposited on Au in 0.1 M H_2SO_4 solution. Their average size was 5 nm. AuNPs were deposited by running CV for 10 cycles as reported by Ehab et al., 2013.[10] We chose the 10 cycle modification time in all experiments to eliminate any complications that may result from producing different surfaces. We also noticed that more deposition deepens the color of the electrode and makes it more difficult to regenerate to a clean gold electrode afterwards. Previous studies showed that small deposition times give reasonable and acceptable modification of the gold electrode with AuNPs.[28] Studying the electrochemical behavior of the electrode, we conclude that there is no significant change in the main reduction peak potential at 8.00E -01 (0.8V) as a function of gold nanoparticles deposition after 10th cycle as shown in figure 1. For further confirmation, A bare gold electrode and an AuNP-modified gold electrode with the same geometric surface areas were characterized by TEM, as shown in figure. S2(A) and (B), respectively. Comparing with figure. S2(A), it can be clearly seen that an average size of 5nm AuNPs has been electrochemically deposited on the surface of the gold electrode.

Fig S1. Cyclic voltammograms of (a) bare GE, (b) AuNPs deposition GE electrode with deposition time of 10 cycles, Electrolyte: aqueous 0.1 M H_2SO_4 solution. Scan rate = 50 mV/s

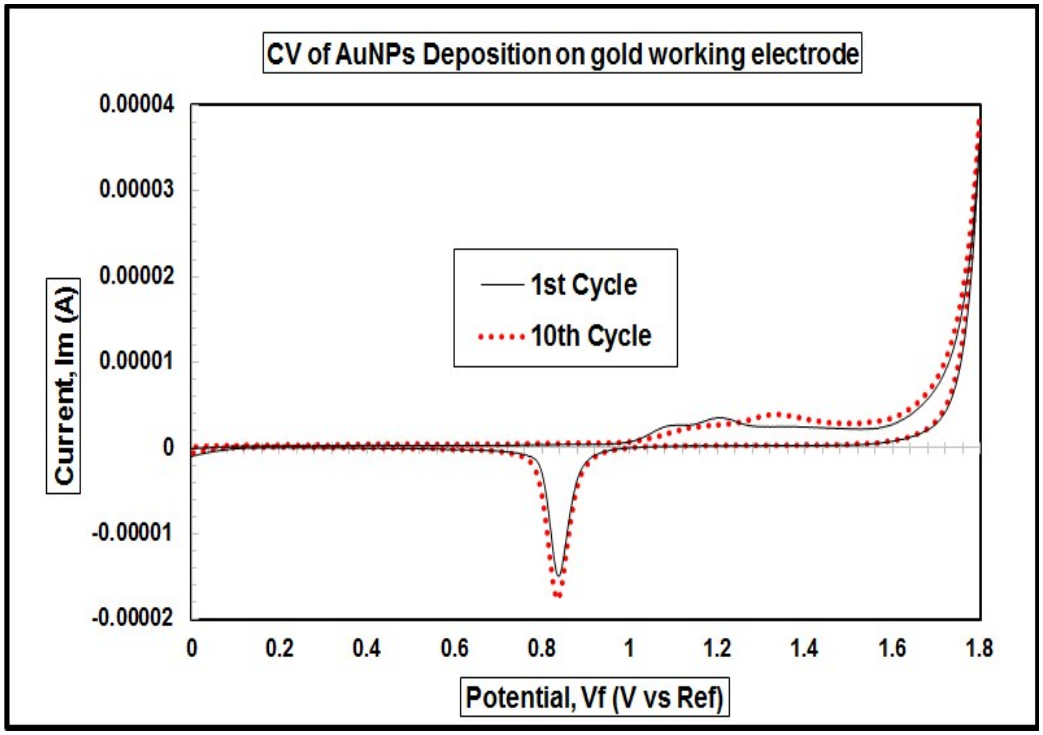

Fig. S2. TEM images of (A) bare gold electrode and (B) AuNPs/gold electrode obtained on 2-3nm Au on 400 mesh Au TEM grid.

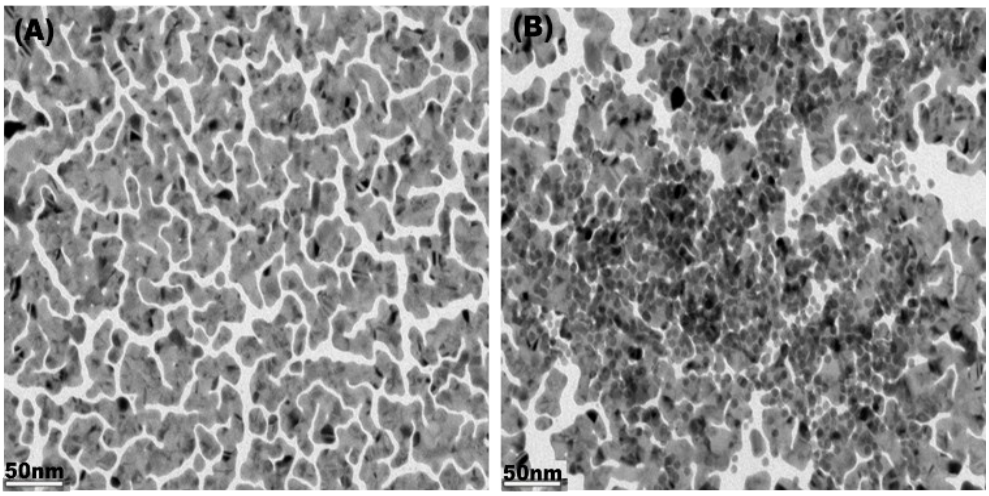

Characterization of aptamer-based biosensor

Fig.S3. Cyclic voltammogram of Aptamer/AuNP/gold electrode with different concentration of IL-6/aptamer/AuNP/gold electrode in 0.5 M PBS containing 5 mM $K_3Fe(CN)_6$ (pH 7.0). Cyclic voltammograms measure the peak current generated by the binding of Aptamer with IL-6 while scanning the dc potential from a starting value to an end value, and reverting back the scan to the initial potential. The peak current was maximum for the highest concentration of IL-6 & lower for lowest concentration of IL-6. All the electrodes used in this work have almost identical CV curves, indicating a good reproducibility of the gold modified electrodes (RSD 3.3%, n = 5).

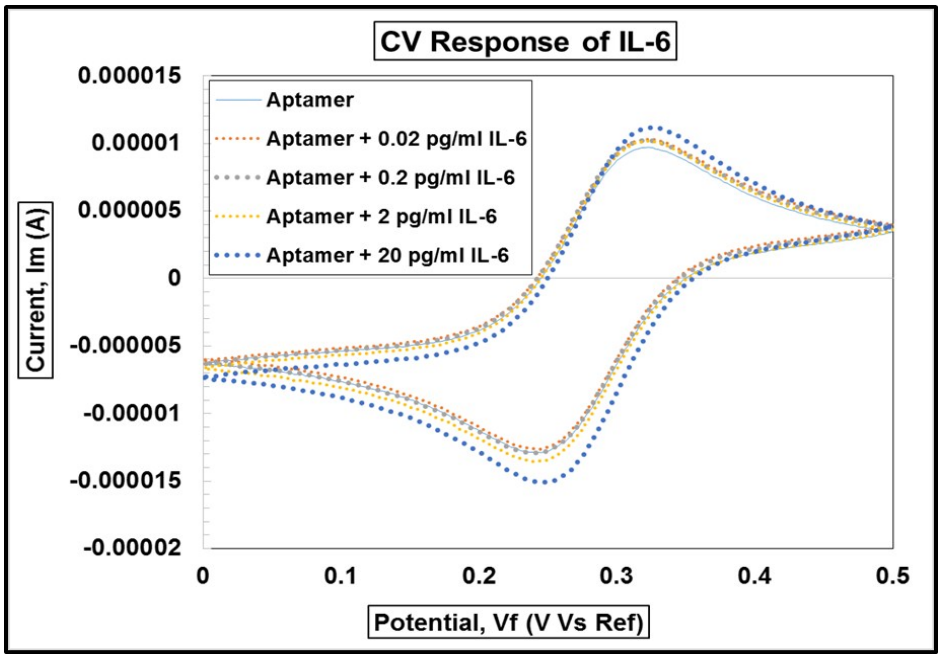

Effect of aptamer optimization on Beacon assay

Different concentrations of functionalized aptamer were taken for their emission at 520nm and excitation at 497nm. Since a concentration more than 0.5 μM of aptamer gave maximum emission intensity, further increase in concentration is not recommended. In order to accommodate either enhancement or quenching of signals after binding with IL-6 protein, a concentration of 0.5 μM of aptamer was selected as optimum concentration to carry out the assay. After an incubation time of 15 min the spectra of the solution with excitation at 497 nm and emission at 520 nm were recorded. The functionalized aptamer in the absence of IL-6 in solution had less fluorescence due to its native conformation, whereas in the presence of IL-6 the fluorescence emission of the aptamer enhances to a higher level. The functionalized aptamer being very specific to IL-6 undergoes binding by the induced fit binding mechanism and leads to a change in the structural conformation of the aptamer. In the native aptamer, the structure of the aptamer brings the ends closer together much below the Forster radius where the emission of the FAM molecule at the 3' end lies in the absorption range of BHQ at the 5' end. The energy from FAM is transferred to BHQ and is quenched, therefore the final emission decreases. Whereas after binding with IL-6, the terminal moves apart and results in an increase in fluoresce signals.

Fig.S4. Aptamer Beacon Assay. Plot of relative fluorescence unit versus log of IL-6 concentration from 0.2 μg/ml to 200 μg/ml . Data were derived from quintuplets assays (n = 5) with error bars of 5%.

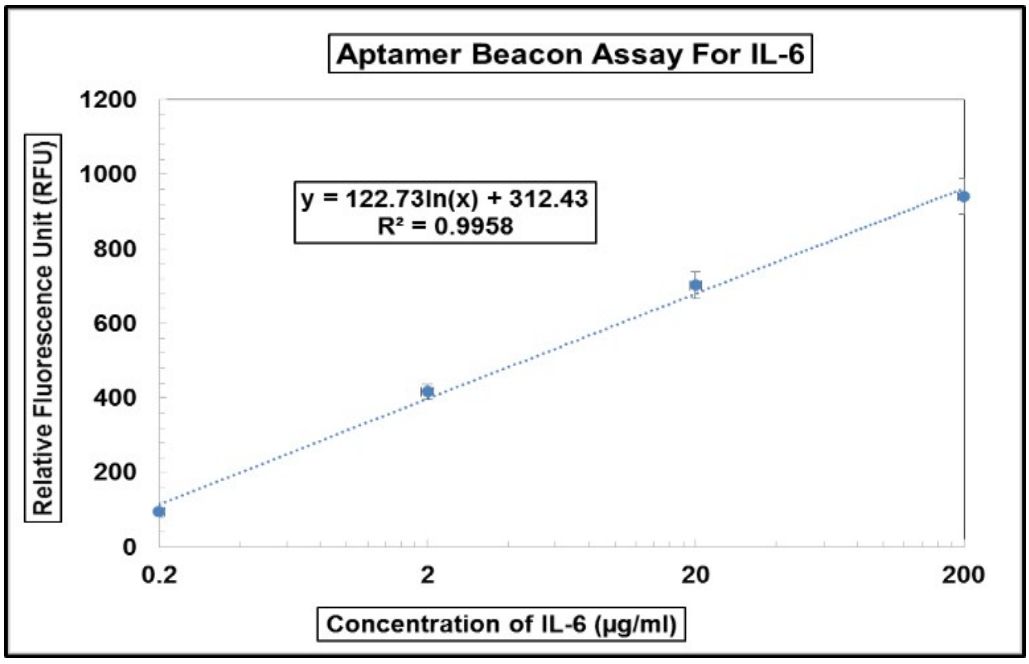

EIS Response for IL-6 in commercial artificial sweat

Fig.S5. Nyquist plots of impedance spectra of IL-6 sensing obtained in commercial artificial sweat containing 5mM $K_3Fe(CN)_6$ redox couple at (a) bare gold electrode; (b) AuNPs deposited on gold electrode; (c) 1 µM Aptamer/AuNPs/gold electrode after interaction for 60 min; (d) 0.02 pg/ml of IL-6/1 µM Aptamer/AuNPs/gold electrode; (e) 0.2 pg/ml of IL-6/1 µM Aptamer/AuNPs/gold electrode; (f) 2 pg/ml of IL-6/1 µM Aptamer/AuNPs/gold electrode; (g) 20 pg/ml of IL-6/1 µM Aptamer/AuNPs/gold electrode; Fitted data (solid line).The biased potential was 0.236V. The frequency was scanned from 1 MHz to 1.0 Hz and the amplitude was 5.0mV.

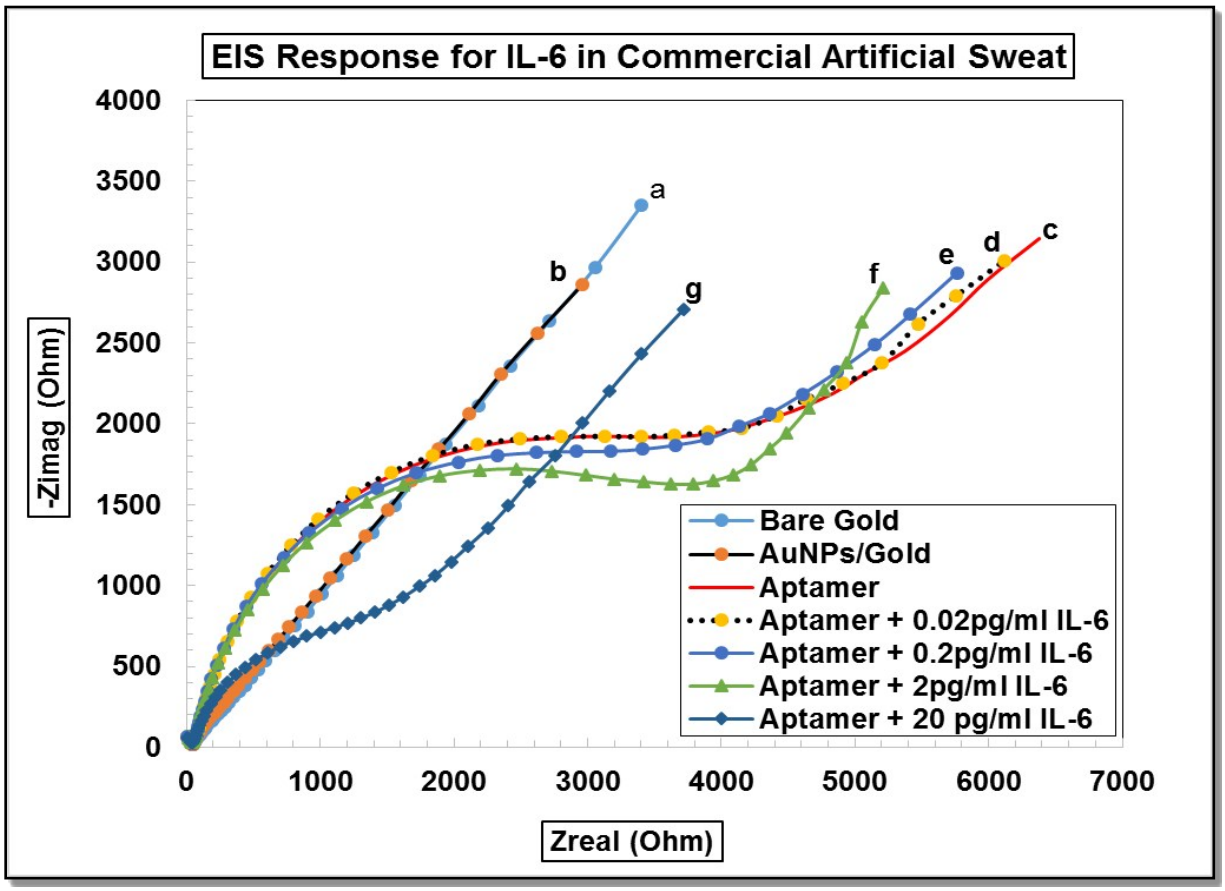

Fig. S6. The storage-time dependence of the relative signal change referring to the original signal of the aptasensor at 0.2 pg/ml IL-6 in the 1st-day measurement. The aptasensor was stored in PBS (pH 7.4,10 mM) at 4°C in a refrigerator.

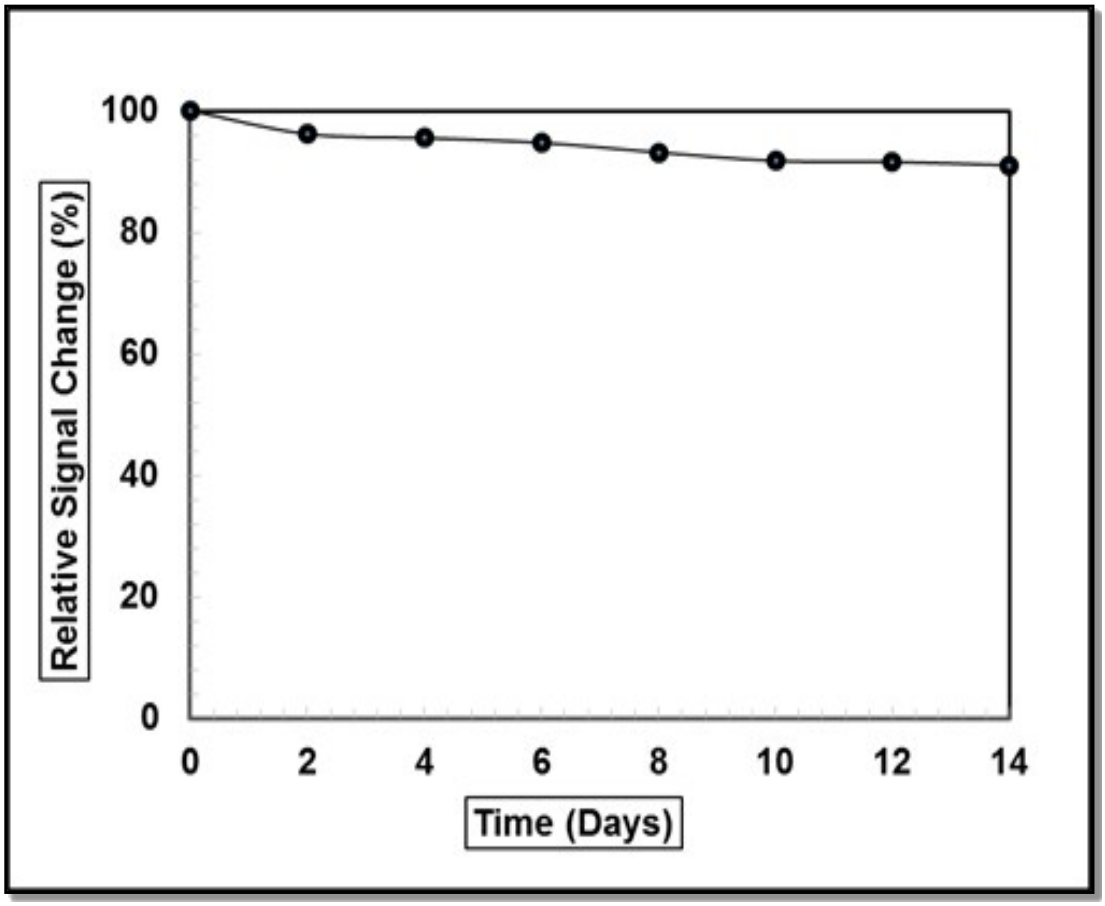

Table S1. Values of the equivalent circuit parameters of the fitting curves for the aptasensor at different fabrication steps includes aptamer/gold electrode after interaction with different concentrations of IL-6 from 0.02 pg/ml to 20 pg/ml.

Fabrication steps	R_s (ohm·cm^2)	R_{et} (ohm·cm^2)	Z_w (S.sec.^5/cm^2)	C (F/ cm^2)
Bare gold electrode	96.11×10^{-6}	40.63	84.01×10^{-6}	17.65×10^{-9}
GNP/gold electrode	3.130×10^{-6}	33.71	105.6×10^{-6}	20.49×10^{-9}
Aptamer/GNP/gold electrode	13.35	10.67×10^{3}	280.2×10^{-6}	4.633×10^{-6}
0.02 pg/ml IL-6/ aptamer/GNP/gold electrode	13.99	10.39×10^{3}	327.3×10^{-6}	4.948×10^{-6}
0.2 pg/ml IL-6/ aptamer/GNP/gold electrode	15.87	7.863×10^{3}	205.7×10^{-6}	5.691×10^{-6}
2 pg/ml IL-6/ aptamer/GNP/gold electrode	14.19	6.872×10^{3}	178.2×10^{-6}	6.070×10^{-6}
20 pg/ml IL-6/ aptamer/GNP/gold electrode	2.428	5.878×10^{3}	136.1×10^{-6}	15.73×10^{-6}

Table S2. Analytical performance of various methods for IL-6 sensors. (Adapted & modified from Gao-Chao Fan et al., 2014). [14]

Method	Linear range	Detection limit	Reference
Goldnanoparticle modified Electrochemical Aptasensor	0.02 -20 pg/ml	0.02 pg/ml	Present work
Aptamer Beacon assay	0.2 – 200 µg/ml	0.2 µg/ml	Present work
Graphene oxide biosensor	4.7 to 300 pg/ml	1.53 pg/ml	[15]
Co-sensitization photoelectrochemistry	0.001–100 ng/ml	0.38 pg/ml	[14]
Electrochemical immunoassay based on screen printing electrode	0.001 to 1000 ng/ml	0.1 pg/ml	[16]
Electrochemical impedance sensor	0.01 to 100 fg/ ml	10 pg/ml	[17]
Silver nanoparticle-hollow titanium phosphate sphere hybrid as a label for ultrasensitive electrochemical detection	0.0005–10 ng/ml	0.1 pg/ml	[18]
Electrochemical sensor utilizing ferrocene loaded porous polyelectrolyte nanoparticles	0.002–20 ng/ml	1 pg/ml	[19]
Electrochemical immunosensor	0.004–0.800 ng/ml	1 pg/ml	[20]
Combination tapered fiber-opticbiosensor	0.12–120 ng/ml	120 pg/ml	[21]
Conductimetric immunosensor	0.025–0.4 ng/ml	5 pg/ml	[22]
Fluorescent microarray	0.1–10 ng/ml	100 pg/ml	[23]
Chemiluminescence imaging assay	0.002–0.3120 ng/ml	5 pg/ml	[24]
ELISA	0.039–2.5 ng/ml	39 pg/ml	[25]

References

1 J. J. Shi, T. Ting, F. Jiang, E.S. Abdel-Halim, J.J. Zhu., *Biosens Bioelectronics* 2014,**55**, 51–56.
2 G. C. Fan, X.L. Ren, C. Zhu, J. R. Zhang, J.J. Zhu., *Biosens. Bioelectronics* 2014, **59**, 45-53.
3 T. Yanga, S. Wanga, H. Jin, W. Bao., S. Huang., J. Wang., *Sens Actuators* 2013, **B178**, 310– 315.
4 G. Wang, H. Huang, G. Zhang, X. Zhang., B. Fang., L. Wang, Langmuir, 2011, **27** (3), 1224-1231
5 Ting Li., Minghui Yang., Sensors. Actuators B-chem 2011, **158 (1)**, 361-365.
6 J. Peng, L.N. Feng, Z.J. Ren, L.P. Jiang, J.J. Zhu, Small 2011,**20**, 2921–2928.
7 J.W.A. Findlay, W.C. Smith, J.W. Lee, J.Pharm.Biomed. Anal 2000,**21**,1249–1273.
8 A.M. Hawkridge, D.C.Muddiman, *Ann.Rev.Anal.Chem* 2009, **2**,265–277.
9 S.M. Hanash, S.J. Pitteri, V.M. Faca, *Nature* 2008, **452**,571–579.
10 E. AlShamaileh, H. Saadeh., V. Favry., *J. Chem.* 2013,**383921**, 5.
11 M.C. Rodriguez, A.N. Kawde, J. Wang, *Chem. Commun* 2005, **34**, 4267–4269.
12 Y. Xiao, A.A. Lubin, A.J. Heeger, K.W. Plaxco, *Angew Chem Int Ed Engl* 2005, **44**, 5456–5459.
13 A.E. Radi, J.L.A. Sanchez, E. Baldrich, C.K. O'Sullivan, J Am Chem Soc 2006,**128**,117–124.
14 F. Gao-Chao, R. Xiao-Lin, Cheng Zhu., Z. Jian-Rong, Z.Jun-Jie, Biosens. Bioelectron. 2014,**59**, 45–53.
15 Jingfeng Huang, Hu Chen, Wenbin Niu, W. H. Derrick Fam, Alagappan Palaniappan, Melanie Larisika, H. Steve Faulkner, Christoph Nowak, Myra A. Nimmo, Bo Liedberg , Alfred I. Y. Tok. RSC Adv, 2015, **5**, 39245-39251.
16 Jian-Jun Shi., Ting-Ting., Fang Jiang, E.S. Abdel-Halim, Jun-Jie Zhu., Biosens Bioelectron 2014,**55**, 51–56.
17 Ting Yanga., Shun Wanga., Huile Jin., Weiwei Bao., Shaoming Huang., Jichang Wang., Sens Actuators, 2013, **178**, 310– 315.
18 J. Peng, L.N. Feng, Z.J. Ren, L.P. Jiang, J.J. Zhu, *Small*, 2011, **20**, 2921–2928.
19 Ting Li, Minghui Yang., *Sensors. Actuators B-chem* 2011,**158** (1), 361-365.
20 G.F. Wang, H. Huang, G. Zhang, X.J. Zhang, B. Fang, L. Wang, Langmuir, 2011, **27**, 1224–1231.
21 C.W. Wang, U. Manne, V.B. Reddy, D.K. Oelschlager, V.R. Katkoori, W.E. Grizzle, R. Kapoor, *J Biomed Opt*. 2010,**15(6)**, 067005.
22 K.Z. Liang, J.S. Qi, W.J. Mu, Z.X. Liu. *Bioprocess Biosyst Eng*. 2009,**32(3)**, 353-359.
23 H. Wu, Q. Huo, S. Varnum, J. Wang, G. Liu, Z. Nie, J. Liu, Y. Lin. *Analyst*. 2008,**133(11)**, 1550–1555.
24 L. Luo, Z. Zhang, L. Hou, *Anal Chim Acta*. 2007, **584(1)**,106-111.
25 C.K. Turner, T.M. Blieden, T.J. Smithc, S.E. Feldon, D.C. Foster, P.J. Sime, R.P. Phipps. *J. Immunol. Methods*, 2004, **291**, 63–70.